Molecular Orientation Effects in a Surface-Confined, Free-Radical Reaction

A. C. Buchanan, III,* Michelle K. Kidder, and Phillip F. Britt

Chemical Sciences Division,Oak Ridge National Laboratory, Oak Ridge, Tennessee 37831-6197

Received: June 29, 2004; In Final Form: August 10, 2004

Molecular confinement on solid surfaces can have important consequences for chemical reactivity. Pyrolysis of silica-immobilized 1,3-diphenylpropane (DPP) at 375 °C has been examined in the presence of a series of isomeric (by point of attachment) co-attached hydroaromatic spacer molecules to explore the role of molecular orientation on a free-radical reaction under surface confinement. The DPP pyrolysis rate was found to be sensitive to both the structure of the spacer and its attachment orientation to the surface. Spacer molecules with a meta orientation of the benzylic hydrogens with respect to the surface linkage were found to produce faster reaction rates than the corresponding para-oriented spacers. Molecular modeling indicates that the meta-attached spacers are better able to attain a favorable separation and geometry for hydrogen transfer to intermediate surface-confined benzyl radicals in the hydrogen transfer, radical relay mechanism on the surface. These orientation effects have important implications in many fields including catalysis, solid-phase synthesis, and the design and preparation of new nanostructured materials.

Introduction

The impact of organic molecular confinement in crystals, in nanoporous solids, or on metal and semiconductor surfaces is being widely investigated as a consequence of the novel chemical and spectroscopic behavior that can result.[1] The knowledge derived from these fundamental studies has important applications in many areas such as catalysis, separations, solid-phase synthesis, sensor design, and the synthesis of nanostructured materials.[1,2] Organic radical chemistry on surfaces continues to draw considerable attention.[1a,b,e,3] An important focus of this chemistry in recent years has been surface initiated radical polymerization for formation of polymer brushes[4] and the synthesis of other organic−inorganic hybrid nanostructures.[5]

We have been exploring the impact of surface confinement on free-radical reactions on silica surfaces both on nonporous nanoparticles (Cabosil, 12 nm)[6] and, more recently, in tunable pore size mesoporous materials (MCM-41, SBA-15).[7] Organic molecules are covalently immobilized to the silica surfaces by condensation of phenols with the surface silanols to generate a $Si-O-C_{aryl}$ linkage. Surface coverage can be controlled through variations in the initial amounts of organic molecules relative to the surface silanol population. Two-component systems are also readily synthesized in controllable compositions in a single step using a mixture of phenols.[6a] The silyl ether surface linkage is thermally stable to ca. 550 °C, permitting the study of high-temperature organic radical reactions. An additional benefit of this linkage relative to the siloxane linkage typically employed for immobilizing organic moieties (using silane coupling agents such as silyl chlorides, silyl alkoxides, or silazanes) is the ease with which the organic products on the surface can be retrieved after the reaction by simple cleavage with aqueous base.[6]

Pyrolysis of silica-immobilized 1,3-diphenylpropane (≈DPP, where "≈" denotes a surface-attached species) provides a convenient free-radical probe reaction to examine the influence of the structure of a second "spacer" molecule on the surface reaction. As shown in Scheme 1, pyrolysis at 375 °C produces a simple mixture of products, gas-phase and surface-attached toluene and styrene, in comparable amounts.[8] The underlying free-radical decay pathway is an efficient chain process (kinetic chain lengths exceeding 250) that has been discussed in detail elsewhere.[8] The propagation steps (Scheme 1) involve gas-phase and surface-attached benzyl radicals abstracting hydrogen from ≈DPP to form the toluene products. Fast unimolecular β-scission of the resulting regiochemically distinct radicals, **1** and **2**, forms the styrene products while regenerating the two benzyl radicals. The overall rate of ≈DPP pyrolysis is controlled by the rates of the bimolecular hydrogen transfer steps, which were found to be sensitive to the surface coverage.[8]

Recently, we began an examination of the impact of intervening spacer molecules on the ≈DPP pyrolysis rate on the nonporous Cabosil surface, and found a remarkable sensitivity to the spacer structure.[6a] For example, the ≈DPP conversion rates at 375 °C (and similar surface coverages) alone and in the presence of co-attached *p*-biphenyl [$\approx C_6H_4C_6H_5$, ≈BP], ≈3,5-dimethylbenzene [$\approx C_6H_3(CH_3)_2$, ≈DMB], and *p*-diphenylmethane ($\approx C_6H_4CH_2C_6H_5$, ≈*p*-DPM) were 1.1×10^{-4}, 2.3×10^{-4}, 7.1×10^{-4}, and 38×10^{-4} % s^{-1}. This stands in stark contrast to solution-phase studies where the DPP pyrolysis rate was the same for biphenyl and diphenylmethane diluents.[9] The unique behavior for the surface-immobilized case led us to propose a novel serial hydrogen transfer, radical relay mechanism for spacer molecules that possess reactive benzylic hydrogens (illustrated in Scheme 2 for the diphenylmethane spacer) as the basis for the rate enhancements with these molecules. The relay mechanism was confirmed by rate measurements with additional spacer molecules of varying hydrogen donating abilities, detailed kinetic analysis, and measurement of a full kinetic isotope of 2.7 at 375 °C when *p*-diphenylmethane-d_2 ($\approx C_6H_4CD_2C_6H_5$) was employed as the spacer.[6a] Hence, in these supramolecular assemblies, the organization of the molecules on the surface leads to efficient bimolecular hydrogen transfers, which mitigate the effects of diffusional constraints imposed by immobilization. Recently, a conceptually similar radical relay mechanism was proposed in

* Corresponding author. E-mail: buchananac@ornl.gov.

10.1021/jp047169+ CCC: $27.50
Published on Web 10/01/2004

SCHEME 1: Products from Pyrolysis of Silica-Immobilized 1,3-Diphenylpropane, and Propagation Steps for the Radical Chain Decomposition Mechanism

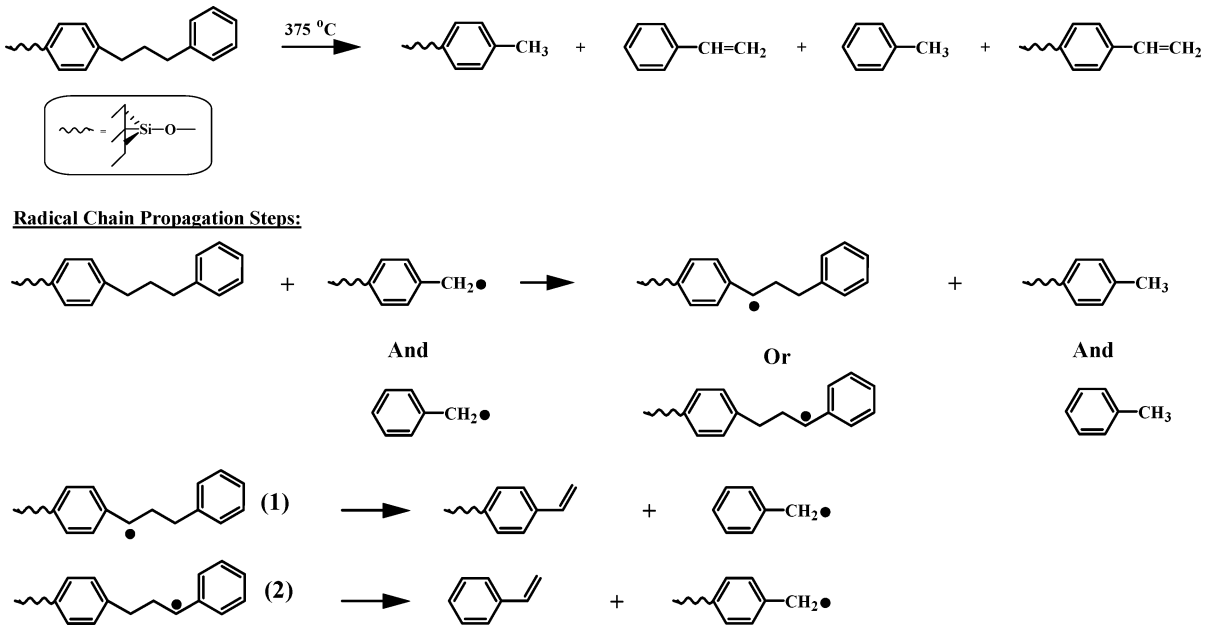

SCHEME 2: Hydrogen Transfer, Radical Relay Mechanism on the Silica Surface

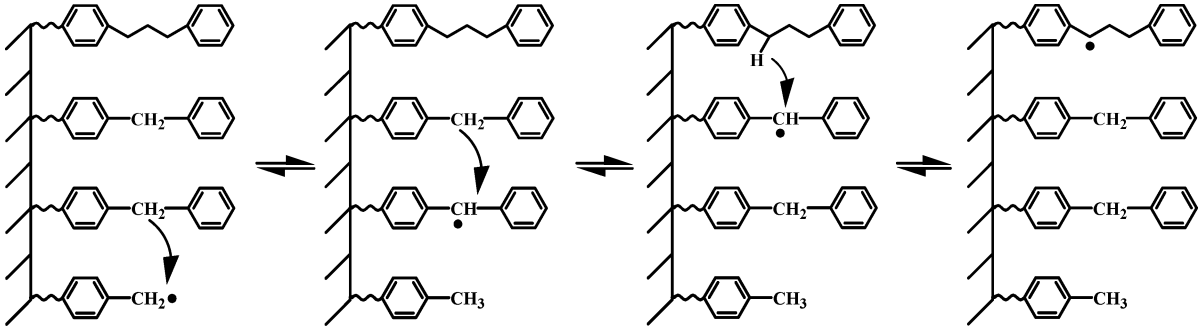

SCHEME 3: Silica-Immobilized Substrates Containing Isomeric Hydrogen Donors That Have Been Synthesized and Subjected to Pyrolysis at 375 °C

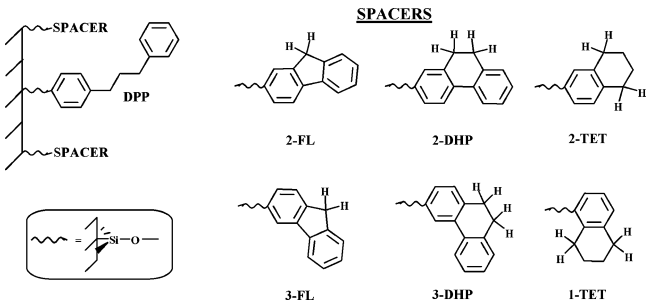

the radical addition−fragmentation chain transfer polymerization of styrene on a related silica surface.[4a] Moreover, Wolkow and co-workers have exploited the related diffusion of dangling bonds (radical sites) on various surfaces of silicon wafers for reactions with alkenes to synthesize new hybrid nanostructures in a manner that is controlled by both the structure of the organic and the silicon surface.[5e−g]

In this paper, we now examine the role of spacer orientation on the ≈DPP pyrolysis rate through study of three pairs of isomeric (by point of surface attachment) hydroaromatic spacers as shown in Scheme 3. Our premise was that if such subtle changes in molecular orientation were to play a role in the high-temperature reactions, they would be most likely revealed in hydroaromatics where the active benzylic hydrogens are locked in a ring. In a recent communication, we reported our initial finding that orientation effects can indeed lead to altered ≈DPP pyrolysis rates.[10] We now present a full account of this work, including new data on rates and product selectivities at different ≈DPP surface dilutions along with additional insights from molecular modeling.

Experimental Section

GC analysis was performed on a Hewlett-Packard 5890 Series II gas chromatograph employing a J & W Scientific 30 m × 0.25 mm DB-5 column (0.25 μm film thickness) and flame ionization detection. Detector response factors were determined relative to cumene (hydrocarbon products) or 2,5-dimethylphenol and *p*-hydroxybiphenyl (phenolic products) as internal standards. Mass spectra were obtained at 70 eV with a Hewlett-Packard 5972A/5890 Series II GC−MS equipped with a capillary column matched to that used for GC analyses.

Materials. Cabosil M-5 silica from Cabot Corp. (200 m^2/g) was dried at 200 °C for 4 h and cooled in a desiccator before use. Benzene was distilled from sodium. High-purity acetone and dichloromethane were commercially available and used as received. Cumene was fractionally distilled (2×), and 2,5-dimethylphenol was recrystallized from ethanol. *p*-Hydroxybiphenyl, 5,6,7,8- tetrahydro-2-naphthol (2-hydroxytetralin, or 2-HOTET), and 5,6,7,8-tetrahydro-1-naphthol (or 1-hydroxyte-

tralin, 1-HOTET) were commercially available and purified by repeated recrystallizations from benzene/hexane.

Synthesis of *p*-(3-phenylpropyl)phenol (HODPP) has been previously described.[8] 2-Hydroxyfluorene (2-HOFL) was synthesized by the Baeyer−Villiger oxidation of 2-fluorenecarboxaldehyde followed by base hydrolysis.[11] 3-Hydroxyfluorene (3-HOFL) was synthesized in several steps beginning with the triflate derivative of 4-methoxy-2-hydroxymethylbenzoate. Suzuki coupling with $PhB(OH)_2$ gave 4-methoxy-2-phenylmethylbenzoate,[12] which was then saponified to form the corresponding carboxylic acid. Treatment with hot polyphosphoric acid resulted in cyclization to form 3-methoxy-9-fluorenone.[13] Wolf-Kishner reduction of the ketone[14] followed by demethylation of the ether with refluxing HBr/acetic acid yielded the desired product. 3-Hydroxy-9,10-dihydrophenanthrene (3-HODHP) was prepared following the method of Takaki.[15] 2-Hydroxy-9,10-dihydrophenanthrene (2-HODHP) was prepared by acetylation of 9,10-dihydrophenanthrene,[16] followed by Baeyer−Villiger oxidation and base hydrolysis.[11] All phenols were purified by multiple recrystallizations from benzene/hexane to purities >99.7%.

Preparation of Surface-Attached Materials. Procedures for the preparation of two-component surfaces have been described previously.[6a,10] In general, HODPP and the desired spacer phenol were dissolved in benzene and added to a benzene slurry containing the dried silica (4.5 g containing ca. 1.5 mmol of SiOH/g). For the HODHP and HOFL isomers, the initial spacer:HODPP mole ratio led to approximately the same ratio of immobilized organics on the surface (±10−15%). For the HOTET isomers a larger initial HOTET:HODPP mole ratio (ca. 3-fold) was required for reasons we do not currently understand. To ensure that all materials contained a saturation coverage of organics, a ca. 2-fold excess of combined HODPP and spacer phenol was employed relative to the total silanol population available. The benzene was removed by evaporation under reduced pressure, and the phenolic material was attached to the silica surface by heating at 225 °C for 1 h in an evacuated (2×10^{-5} Torr) sealed Pyrex tube. Unattached phenols were removed via ramped sublimation at 225−275 °C (10 °C min^{-1}; 20-min hold) under dynamic vacuum (5×10^{-3} Torr). Surface coverage analysis was performed by GC with *p*-hydroxybiphenyl as internal standard as described previously following cleavage of the phenols from the surface by a base hydrolysis procedure.[6a]

Pyrolysis Procedure. The pyrolysis apparatus and procedure have been described.[6,10] In brief, a weighed amount of sample (0.3−0.4 g) was placed in a T-shaped Pyrex tube, evacuated, and sealed at ca. 2×10^{-6} Torr. The sample was pyrolyzed in a preheated calibrated three-zone tube furnace, and the gas-phase products were trapped in the tube arm placed in a liquid nitrogen bath. The volatile products collected in the trap were dissolved in acetone (100 μL) containing cumene as an internal standard, and the solution was analyzed by GC and GC−MS. Surface-attached pyrolysis products were hydrolyzed from the silica with 1 N NaOH, and the internal standards 2, 5-dimethylphenol and *p*-hydroxybiphenyl were added to the solution. The solution was acidified and extracted with CH_2Cl_2, washed with water, dried over $MgSO_4$, and filtered, and the solvent was evaporated. The residue was silylated with ca. 300 μL of *N*,*O*-bis(trimethylsilyl)trifluoroacetamide (BSTFA) in pyridine (1:2 v/v) and analyzed by GC and GC−MS.

The four ≈DPP pyrolysis products shown in Scheme 1 typically accounted for nearly all of the products (>98 mol %), consistent with previous ≈DPP pyrolysis studies with other spacers.[6a] No products (>1%) were detected from the tetralin spacers, while the dihydrophenanthrene spacers gave small quantities (1−2%) of the corresponding dehydrogenated phenanthrene product. In the fluorene case, both isomers showed small quantities of products (3−8%) resulting from addition of fluorenyl radical intermediates to the surface-attached styrene.

SCHEME 4: Synthesis of Two-Component Chemically Modified Silica Surfaces

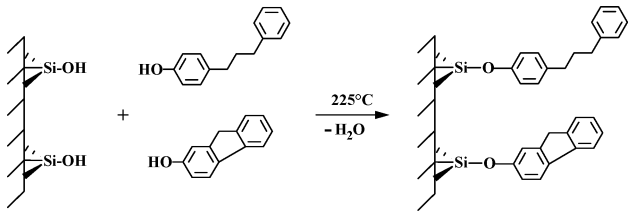

TABLE 1: Two-Component Surfaces Investigated

surface composition	coverage[a] (mmol g^{-1})	coverage[b] (nm^{-2})	spacer:DPP (mol ratio)
≈DPP/≈2-TET	0.11/0.45	0.36/1.47	4.1
	0.11/0.51	0.36/1.68	4.6
≈DPP/≈1-TET	0.11/0.22	0.35/0.70	2.0
	0.085/0.28	0.27/0.89	3.3
	0.051/0.32	0.16/1.02	6.3
≈DPP/≈2-DHP	0.14/0.47	0.47/1.59	3.4
	0.066/0.48	0.22/1.61	7.3
≈DPP/≈3-DHP	0.21/0.36	0.71/1.21	1.7
	0.065/0.47	0.22/1.59	7.2
≈DPP/≈2-FL	0.16/0.43	0.54/1.44	2.7
	0.083/0.50	0.28/1.67	6.0
≈DPP/≈3-FL	0.12/0.33	0.39/1.08	2.8
	0.068/0.40	0.22/1.31	5.9

[a] Surface coverages of the components on a per gram of derivatized silica basis. [b] Surface coverages in molecules per nm^2 surface area for the native silica (200 m^2 g^{-1}).

Results and Discussion

Surface-Attached Materials. The two-component surfaces shown in Scheme 3 were synthesized by the co-condensation of the precursor phenols with the surface silanols of the Cabosil in a single step as illustrated in Scheme 4. ≈DPP and spacer surface coverages are shown in Table 1 on a millimole per gram of derivatized silica basis (column 2). In column 3, the surface coverages are calculated on a molecules per square nanometer surface area basis. The ratio of spacer to DPP surface coverage (column 4) is controlled by the initial ratio of precursor phenols, while saturation surface coverages are achieved through the use of excess phenol compared with the silica silanol population (see Experimental Section). The total surface coverages obtained (1.5−2.0 molecules nm^{-2}) are consistent with the saturation surface coverages obtained previously for other two-component surfaces.[6a] The exception is the ≈DPP/≈1-TET case, where the total surface coverages are lower (1.1−1.2 molecules nm^{-2}) indicating that the surface is less densely packed for this isomer.

Pyrolysis Products and Selectivity. Pyrolyses were conducted at 375 °C under vacuum in sealed tubes, and gas-phase and surface-attached products were analyzed as described in the Experimental Section. The silica-attached products were analyzed as the corresponding phenols. As shown in Table 2, four to seven pyrolyses were conducted on each sample. The ≈DPP conversions were typically limited to <20% (except for the highly reactive FL spacers) to focus on initial rates and primary products. Total mass balances were excellent, typically exceeding 98 mol %.

Toluene and styrene are formed in both gas-phase and surface-attached forms as shown in Scheme 1, and these four

TABLE 2: Effect of Spacer Structure on ≈DPP Pyrolysis Rate and Product Selectivity at 375 °C

surface composition	coverage (nm^{-2})	spacer:DPP (mol ratio)	no. of pyrolyses	≈DPP conversion range (%)	rate × 10^4 [a] (% s^{-1})	correlation (R^2)[b]	selectivity[c]
≈DPP/≈2-TET	0.36/1.47	4.1	7	4.2−16.9	42	0.992	0.92
	0.36/1.68	4.6	6	3.7−13.6	41	0.988	0.93
≈DPP/≈1-TET	0.35/0.70	2.0	4	3.3−9.4	15	0.996	1.18
	0.27/0.89	3.3	6	1.9−9.2	15	0.990	1.14
	0.16/1.02	6.3	5	3.9−11.4	13	0.996	1.14
≈DPP/≈2-DHP	0.47/1.59	3.4	6	4.5−11.4	21	0.978	0.86
	0.22/1.61	7.3	6	6.1−11.8	19	0.954	0.84
≈DPP/≈3-DHP	0.71/1.21	1.7	5	1.7−9.1	8.6	0.972	0.85
	0.22/1.59	7.2	4	3.5−19.1	9.3	0.992	0.89
≈DPP/≈2-FL	0.54/1.44	2.7	5	9.4−35.6	201	0.988	0.89
	0.28/1.67	6.0	4	4.2−36.9	219	0.998	0.86
≈DPP/≈3-FL	0.39/1.08	2.8	5	5.6−22.0	82	0.996	0.92
	0.22/1.31	5.9	5	7.1−19.9	103	0.994	0.92

[a] Initial rates determined from the slopes of linear regressions of ≈DPP conversion versus reaction time. Error in rates is ±10%. [b] Square of correlation coefficients for the regression analysis of the rate plots. [c] Pyrolysis selectivity defined by the average of the yield ratios, $PhCH{=}CH_2$/$PhCH_3$. Error in selectivity values is ±3%.

products typically account for >98 mol % of the products. The radical chain propagation steps are also shown in Scheme 1. Since the β-scission steps for radicals **1** and **2** are fast compared to the hydrogen transfer steps, any regioselectivity in the pyrolysis reaction will result from the relative rates for formation of **1** and **2**. Radical **1** is expected to be slightly more stable than **2** as a consequence of the stabilizing effect of the *p*-silyloxy surface linkage.[8] We define the reaction selectivity, *S*, as the ratio of the styrene to toluene yields in the gas phase, which is a measure of the selectivity for formation of **2** relative to **1** (Scheme 1). As a reference point, pyrolysis of the related *p*-$(CH_3)_3SiOPh(CH_2)_3Ph$ at 375 °C in fluid phases gave a value of $S = 0.91$, consistent with a small substituent effect for the *p*-silyloxy group favoring formation of the analogue of **1**.[17] In our previous study, we found that a good hydrogen donor spacer such as ≈DPM gave $S = 0.91$ while aromatic spacers such as biphenyl and naphthalene resulted in $S = 1.09-1.14$.[6a] The effect of the non-hydrogen donating aromatic spacers is thus a subtle shift in regioselectivity favoring hydrogen abstraction at the more accessible benzylic site farthest from the surface that produces radical **2**.

The selectivity values for the spacers studied in the current work are listed in Table 2. The selectivities for a given spacer show no dependence on the spacer:≈DPP ratio. For the ≈FL and ≈DHP spacers, there is no measurable distinction between the isomers and the selectivity values of ca. 0.9 are consistent with our previous results for the ≈DPM hydrogen donating spacer. Likewise, the selectivity values for the ≈2-TET spacer, $S = 0.92-0.93$, fit this trend. However, a larger value of $S = 1.15-1.18$ was measured for the ≈1-TET spacer, indicating a slight preference for formation of radical **2** in contrast to the other spacers. The origin of this effect is not certain, but we noted above that ≈DPP/≈1-TET surfaces formed the least dense saturation surface coverages (ca. 1.1 molecules nm^{-2}) compared with the other materials (ca. 1.5−2.0 molecules nm^{-2}). For hydrogen transfers between ≈DPP and surface-bound radicals, this decreased surface coverage could result in increasing probability that hydrogen abstraction will occur at the more accessible benzylic site in ≈DPP that is farthest from the surface. In support of this premise, previous studies of single-component surfaces of ≈DPP (no spacers) as a function of initial ≈DPP surface coverage showed that *S* increased as the surface coverage decreased.[8] However, our molecular modeling studies (vide infra) were unable to shed any light on this issue, because of the many conformations available to ≈DPP and the benzylic radicals of ≈1-TET, and more sophisticated computational studies will be required.

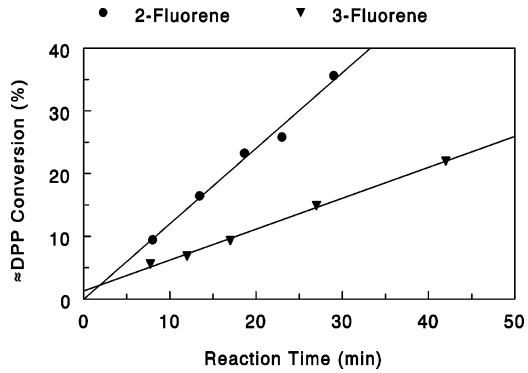

Figure 1. Measurement of reaction rate for ≈DPP. Pyrolysis in the presence of ≈2-FL and ≈3-FL spacers at a spacer:DPP ratio of 2.7 and 2.8, respectively.

Reaction Rates. The initial rates for ≈DPP pyrolysis at 375 °C were obtained from the slopes of the linear regressions of ≈DPP conversion versus reaction time. An example is shown in Figure 1 for the case of the ≈2-FL and ≈3-FL spacers at a spacer:DPP surface coverage ratio of ca. 2.7. The reaction rates and the R^2 values for the linear regressions for all surfaces studied are presented in Table 2. It is immediately evident from the plot in Figure 1 that the reaction rate is substantially different for the two isomeric fluorene spacers. The ≈2-FL spacer, which has a meta orientation of the surface linkage with respect to the benzylic hydrogens, is ca. 2.3 times faster. This is contrary to predictions based on stereoelectronic considerations, since the ≈3-FL spacer with the *p*-silyloxy surface linkage would be expected to generate a more stable benzylic radical intermediate on the fluorene and, hence, a faster reaction rate. In fact, previously we found that the ≈DPP pyrolysis rate in the presence of diphenylmethane isomeric spacers was ca. 40% faster for the para isomer compared with the meta isomer.[6a] The origin of this unexpected orientation effect for the ≈FL spacers will be discussed in more detail below.

To further examine the generality of these surface orientation effects, isomers of two other hydroaromatic spacers were examined that have different hydrogen donating abilities to radicals (vide infra). As seen in Table 2, there are distinct differences in the reaction rates for the isomers of the ≈DHP and ≈TET spacers. The rate was ca. 2.8 times faster for the ≈2-TET spacer than for ≈1-TET, and ca. 2.4 times faster for ≈2-DHP compared with ≈3-DHP. We were also interested to see if the reaction rates were sensitive to the amounts of spacer present relative to ≈DPP, and examined reactions with

TABLE 3: Correlation of ≈DPP Pyrolysis Rates with Hydrogen Transfer Rates at 375 °C

H-donor spacer	avg pyrolysis rate × 10^4 [a] (% s^{-1})	rel pyrolysis rate per H[b]	rel H-transfer rate per H[c]
≈3,5-DMB[d]	7.1	1.0	1.0
≈*m*-DPM[d]	27	11.4	7.3
≈*p*-DPM[d]	38	16.0	
≈2-TET	42	8.9	7.5
≈1-TET	14	3.0	
≈2-DHP	20	4.2 (8.4)[e]	11.5
≈3-DHP	9.0	1.9 (3.8)[e]	
≈2-FL	210	89.0	80.5
≈3-FL	92	39.0	

[a] Average ≈DPP pyrolysis rate for all surface coverages (see Table 2). [b] ≈DPP pyrolysis rates are normalized for the number of benzylic hydrogens except where noted. Rates are then normalized to the ≈3,5-DMB spacer. [c] Relative rates for hydrogen transfer in solution from the corresponding hydrogen donor to the 2-allylbenzyl radical.[19] Rates are extrapolated from 160 °C using Arrhenius parameters for DMB, DPM, and FL, while the DHP and TET rates are extrapolated relative to DPM. [d] Data for DMB (dimethylbenzene) and DPM (diphenylmethane) are from ref 6a. [e] Values in parentheses assume only two benzylic hydrogens are involved.

spacer:≈DPP ratios as high as 7.3. The data in Table 2 show that, for a given spacer, the reaction rate is insensitive to this ratio at the saturation surface coverages of organics that were employed. Undoubtedly, if the total organic surface coverage were decreased, the ≈DPP pyrolysis rate would decrease. This has been documented in previous studies of single-component surfaces of ≈DPP.[8] However, the lack of dependence of the rate on the spacer:≈DPP ratio is testimony to the efficiency of the hydrogen transfer, radical relay mechanism (Scheme 2) at saturation surface coverages, and suggests that the radical relay mechanism can occur over sizable domains of surface-bound hydroaromatic spacers before termination.[18]

Dependence of Pyrolysis Rates on Hydrogen Transfer Kinetics. The ≈DPP pyrolysis rates for the hydroaromatic spacers in Table 2 have been averaged and are collected in Table 3, along with the rates previously measured for the 3,5-dimethylbenzene and diphenylmethane spacers.[6a] The rates at 375 °C are quite sensitive to both the structure of the spacer molecule and its orientation on the surface. The ≈DPP rates vary from 7.1×10^{-4} % s^{-1} for the ≈3,5-DMB spacer to ≈210×10^{-4} % s^{-1} for the ≈2-FL spacer. This rate variation of ca. 30-fold increases to ca. 90-fold when the rate for the non hydrogen donating biphenyl spacer, 2.3×10^{-4} % s^{-1}, is included.[6a]

The structural dependence of the rate variation is rooted in the kinetics of hydrogen donation by the spacer molecules to the gas-phase and surface-attached benzyl radicals. To analyze this in more detail, the rates of ≈DPP/≈spacer pyrolysis are calculated relative to the ≈3,5-DMB spacer and normalized for the number of benzylic hydrogens (Table 3, column 3). For the ≈TET spacers, we make the usual assumption that only the benzylic hydrogens are active.[19] In the case of the ≈DHP spacers, molecular modeling (vide infra) suggests that only two of the benzylic hydrogens are accessible to surface-bound benzyl radicals, and this calculation produces the larger numbers in parentheses. In solution, the rate constants for hydrogen transfer from the corresponding hydrocarbon to the 2-allylbenzyl radical have been measured at 160 °C.[19] Extrapolation of these numbers to 375 °C and normalization for the number of benzylic hydrogens give the relative rates shown in Table 3, column 4. A linear correlation with near unit slope exists between the ≈DPP pyrolysis rates on the surface for the ≈DMB, ≈*m*-DPM, ≈2-TET, ≈2-DHP, and ≈2-FL spacers, which contain meta-type linkages to the surface, and the solution-phase hydrogen transfer rate constants. The slopes/R^2 values for the correlations assuming two or four active benzylic hydrogens for the ≈2-DHP spacer are similar, 1.10/0.994 and 1.11/0.986, respectively. This correlation further confirms the critical importance of hydrogen transfer from the spacers to chain carrying benzyl radicals in determining the ≈DPP pyrolysis rate. Since the correlation involves four closely spaced points and one that is significantly different, the slope value depends strongly on this single point. However, the correlation suggests that solution-phase Arrhenius parameters for hydrogen transfer can be used to predict ≈DPP pyrolysis rates in the absence of geometric constraints. Additional data with other hydrogen donors would be beneficial to confirm this hypothesis. The perhaps surprisingly large increase in rate going from diphenylmethane to fluorene as the hydrogen donor is principally a consequence of the fact that the cyclic fluorene molecule does not require phenyl bond rotations to be frozen out in the transition state for hydrogen transfer.

As discussed above, the rates for the ≈3-FL and the ≈3-DHP spacers, which have para-type linkages to the surface, are ca. 2.3 times slower than their counterparts with meta linkages, contrary to predictions based on substituent effects. In the next section, molecular modeling studies are conducted to provide some insights into the origin of these effects. The ≈2-TET (*m*- and *p*-benzylic methylenes) and ≈1-TET (*o*- and *m*-benzylic methylenes) are not as readily compared and will not be discussed.

Molecular Modeling Studies. Previous NMR studies have shown that the surface of amorphous, nonporous Cabosil silica consists predominantly of isolated, Q3, silanol sites with the remainder being of the geminal, or Q2, type.[20] The [111] and [100] surfaces of β-cristobalite can be used to construct models of the isolated and geminal hydroxyl domains, respectively, in Cabosil.[20] We recently developed small models of these surfaces to aid in examining the rotational dynamics of silica-immobilized aromatic molecules on Cabosil.[21] In the current study, the model of the [111] surface will be employed to explore the molecular orientation effects on the pyrolysis rates described above. The molecular mechanics modeling methodology using the MM+ force field (Hyperchem, V5.0; Hypercube, Inc.) has been described previously.[21]

The most straightforward comparison is for the two ≈FL isomers which have a single methylene carbon that can be involved in hydrogen transfer. Presumably, the mobile gas-phase benzyl radical will not show any significant preference for the orientation of the ≈FL spacer molecule, outside of the small substituent effect favoring the ≈3-FL isomer (vide supra), and the rate difference favoring the ≈2-FL over the ≈3-FL spacer can be attributed primarily to the hydrogen transfer step involving the surface-immobilized benzyl radical. A comparison of the hydrogen transfer for the two spacers is shown in Figure 2. The [111] surface of β-cristobalite contains 4.55 single SiOH's nm^{-2} in a hexagonal array. The models are shown with the benzyl radical in the center surrounded by three neighboring fluorene molecules at a separation (O−O) of 0.5 nm. The fluorenes are separated by 0.87 nm (O−O), corresponding to a 1.5 molecules nm^{-2} coverage, similar to the measured surface coverage.[22] Hence, these simplified models provide a reasonable representation of the saturation surface coverages employed in the pyrolysis studies.

Rotations about the Si−O and the O−C_{aryl} bonds reveal that the meta linkage associated with the ≈2-FL spacer provides a more favorable separation and geometry for the hydrogen

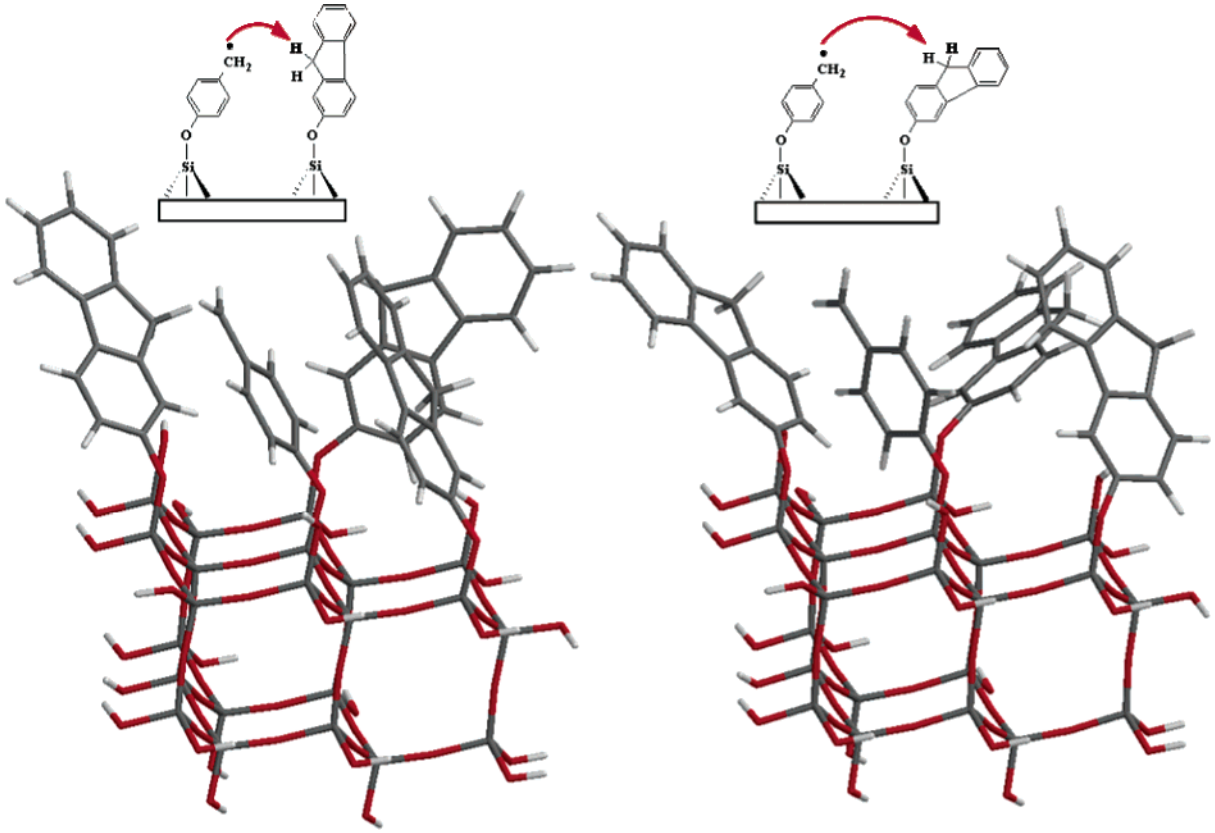

Figure 2. Molecular model of hydrogen abstraction by benzyl radical from the ≈2-FL (left) and the ≈3-FL (right) spacers on the [111] surface of β-cristobalite. The benzyl radical is shown surrounded by three neighboring fluorene molecules with a 0.50 nm separation (O−O).

transfer to occur than the para linkage associated with the ≈3-FL spacer. Recent high-level theoretical calculations on hydrogen abstraction reactions by methyl radical have given a C_{rad}−H separation of ca. 1.35 Å in the transition state for several substituted alkanes.[23] In the benzyl radical hydrogen abstractions shown in Figure 2, this C_{rad}−H separation is easily achieved for the ≈2-FL case (the separation shown in the figure is ca. 1.0 Å). In the case of the ≈3-FL, a C_{rad}−H separation of ca. 1.4 Å can occur for the hydrogen abstraction, but with some steric interferences with neighboring fluorene molecules on the surface. Of course, at 375 °C, there will be considerable molecular motion to overcome some of these steric constraints, but the models clearly suggest that the faster rate for the ≈2-FL can be attributed to a better geometry for hydrogen transfer to the benzyl radical afforded by the meta linkage. Examination of models of the other isomeric spacers leads to a similar conclusion.

Once the hydrogen abstraction occurs to generate the surface-immobilized toluene product and the fluorenyl radical intermediate, further hydrogen transfers must occur between the spacer molecules to permit the relay process depicted in Scheme 2 to occur. According to the model and the saturation surface densities of the spacers employed, this hydrogen transfer will generally occur between spacers that are next nearest neighbors with an O−O separation of 0.87 nm rather than the 0.5 nm separation that exists for nearest neighbors. This is readily achieved for the fluorene spacers as shown in Figure 3 for the ≈2-FL case, which has a 1.4 Å C_{rad}−H separation between the carbon-centered radical and the benzylic hydrogen of the next nearest neighbor fluorene molecule. These results provide further support for the efficacy of the hydrogen transfer, radical relay mechanism with the hydrogen donating spacer molecules.

In our analysis of the correlation of ≈DPP/≈spacer pyrolysis rates with the rates of hydrogen transfer to benzyl radicals, we

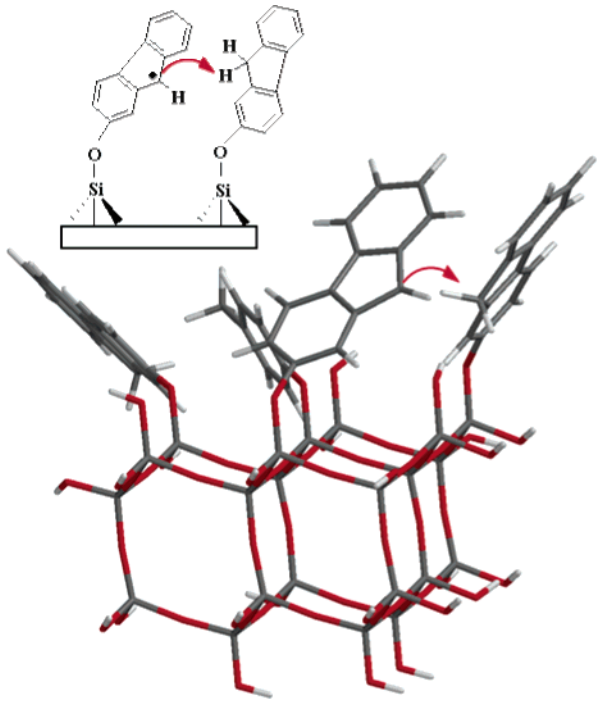

Figure 3. Hydrogen abstraction by the fluorenyl radical from a second fluorene spacer molecule (≈2-FL case) at a separation of 0.87 nm (O−O).

initially assumed that all benzylic hydrogens were actively involved in the hydrogen transfer to the surface-attached benzyl radicals. However, models of the surfaces containing the ≈DHP spacers indicate that only the benzylic methylene that is meta to the surface linkage can be involved in the hydrogen transfer to an adjacent benzyl radical. This is illustrated in Figure 4 for

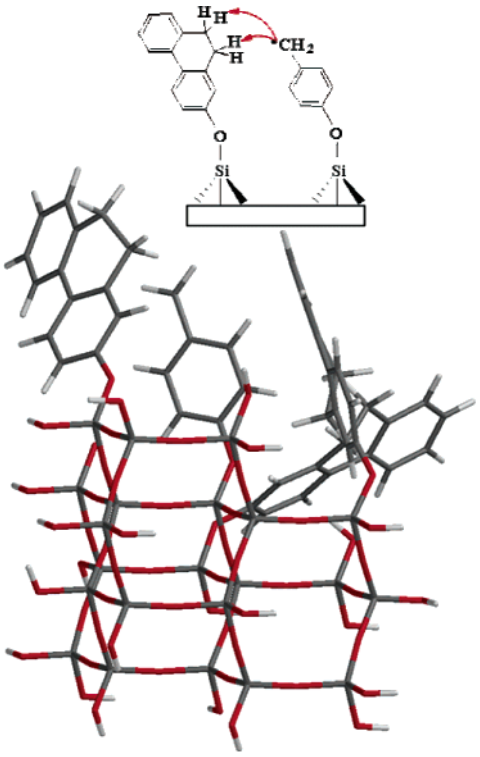

Figure 4. Hydrogen abstraction by the benzyl radical from ≈2-DHP. Only the two nearest hydrogens on the ≈2-DHP are accessible.

the benzyl radical abstracting hydrogen from ≈2-DHP, where the $C_{rad}-H$ separation shown is ca. 1.4 Å. In this configuration, the comparable distances to the other methylene hydrogens are >3.5 Å, which are too far for any probability of hydrogen transfer. It seems likely that all of the spacer benzylic hydrogens would be accessible for hydrogen transfer to the gas-phase benzyl radical. The data given in Table 2 then gives the limits for the correlation, namely involvement by either two or four hydrogens. Experiments involving deuterium labeling of one or the other methylene sites in ≈2-DHP could provide some additional insight into this question.

These simple molecular mechanics modeling studies have assisted in the visualization of the nature of the orientation effects that can occur in radical reactions on surfaces. A more in-depth understanding of these effects would likely require more sophisticated electronic structure and molecular dynamics calculations performed on larger portions of these model silica surfaces.

Conclusions

These studies have advanced our understanding of the important impacts of surface confinement on free-radical reactions. The hydrogen transfer, radical relay pathway that allows radical centers to migrate on the surface by a nondiffusional pathway has important implications not only for understanding chemical reactivity but also for the design of new nanostructured materials, e.g., in the synthesis of nanostructured polymer films grown from surfaces[4a] or the growth of new hybrid organic−silicon nanostructured devices.[5e−g] Our current work on two-component surfaces has examined the effect of isomeric hydrogen donor spacer molecules on the efficacy of the radical relay process. We have shown that subtle changes in the spacer molecular orientation can alter the reaction rate even at high temperatures. Reaction rates could be accelerated nearly 100-fold compared with a non hydrogen donor spacer by the proper choice of hydrogen donor in the best orientation to participate in the relay process, a feature not observed in solution phases.

This behavior is essentially a supramolecular catalysis in which spatial confinement and molecular alignment convert an otherwise bimolecular process into a unimolecular process. The concept of supramolecular catalysis for chemical transformations of two simultaneously complexed molecules in homogeneous phases has recently been reviewed by Mandolini and coworkers.[24] Rate enhancements are similarly discussed in entropic terms and utilize the concept of "effective molarities". The importance of the proper mutual molecular orientation to realize the full rate enhancements is also described. In our studies on silica surfaces, we find that spacer molecules with a meta orientation of the benzylic hydrogens with respect to the surface linkage are able to attain a better geometry for the hydrogen transfer to adjacent benzyl radicals on the surface than spacers with a para orientation. Further extensions of this work to solids with tunable pore sizes and pore surface curvatures, which are important as catalytic supports, are envisioned.

Acknowledgment. This research was sponsored by the Division of Chemical Sciences, Geosciences, and Biosciences, Office of Basic Energy Sciences, U.S. Department of Energy, under Contract No. DE-AC05-00OR22725 with Oak Ridge National Laboratory, managed and operated by UT−Battelle, LLC.

References and Notes

(1) (a) Turro, N. J. *Chem. Commun.* **2002**, 2279. (b) Rouhi, A. M. *Chem. Eng. News* **2000**, Aug 21, 40. (c) Joy, A.; Uppili, S.; Netherton, M. R.; Scheffer, J. R.; Ramamurthy, V. *J. Am. Chem. Soc.* **2000**, *122*, 728. (d) Tung, C.-H.; Wu, L.-Z.; Zhang, L.-P.; Chen, B. *Acc. Chem. Res.* **2003**, *36*, 39. (e) Nagl, I.; Widenmeyer, M.; Grasser, S.; Kohler, K.; Anwander, R. *J. Am. Chem. Soc.* **2000**, *122*, 1544. (f) Sivaguru, J.; Natarajan, A.; Kaanumalle, L. S.; Uppili, S.; Joy, A.; Ramamurthy, V. *Acc. Chem. Res.* **2003**, *36*, 509.

(2) (a) McKitrick, M. W.; Jones, C. W. *J. Am. Chem. Soc.* **2004**, *126*, 3052. (b) Lummerstorfer, T.; Hoffman, H. *J. Phys. Chem. B* **2004**, *108*, 3963. (c) Moineau, J.; Granier, M.; Lanneau, G. F. *Langmuir* **2004**, *20*, 3202. (d) Thomas, A.; Polarz, S.; Antonietti, M. *J. Phys. Chem. B* **2003**, *107*, 5081. (e) Gambs, C.; Dickerson, T. J.; Mahajan, S.; Pasternack, L. B.; Janda, K. D. *J. Org. Chem.* **2003**, *68*, 3673.

(3) (a) Turro, N. J.; Lei, X.-G.; Jockusch, S.; Li, W.; Liu, Z.; Abrams, L.; Ottaviani, M. F. *J. Org. Chem.* **2002**, *67*, 2606. (b) Turro, N. J. *Acc. Chem. Res.* **2000**, *33*, 637. (c) Lee, C.-H.; Lim, T.-S.; Mou, C. Y. *Phys. Chem. Chem. Phys.* **2002**, *4*, 3106. (d) Kretzschmar, I.; Friend, C. M.; Sigman, M. E. *J. Phys. Chem. B* **2002**, *106*, 663. (e) Gu, W.; Warrier, M.; Ramamurthy, V.; Weiss, R. G. *J. Am. Chem. Soc.* **1999**, *121*, 9467. (f) Chen, Y.; Kervio, E.; Rétey, J. *Helv. Chim. Acta* **2002**, *85*, 552.

(4) (a) Tsujii, Y.; Ejaz, M.; Sato, K.; Goto, A.; Fukuda, T. *Macromolecules* **2001**, *34*, 8872. (b) Tomlinson, M. R.; Genzer, J. *Chem. Commun.* **2003**, 1350. (c) Huseman, M.; Morrison, M.; Benoit, D.; Frommer, J.; Mate, C. M.; Hinsberg, W. D.; Hedrick, J. L.; Hawker, C. J. *Langmuir* **2000**, *122*, 1844. (d) Granville, A. M.; Boyes, S. G.; Akgun, B.; Foster, M. D.; Brittain, W. J. *Macromolecules* **2004**, *37*, 2790.

(5) (a) Wang, J.-Y.; Chen, W.; Liu, A.-H.; Lu, G.; Zhang, G.; Zhang, J.-H.; Yang, B. *J. Am. Chem. Soc.* **2002**, *124*, 13358. (b) Blomberg, S.; Ostberg, S.; Harth, E.; Bosman, A. W.; van Horn, B.; Hawker, C. J. *J. Polym. Sci., Part A: Polym. Chem.* **2002**, *40*, 1309. (c) Carrot, G.; Diamanti, S.; Manuszak, M.; Charleux, B.; Vairon, J. P. *J. Polym. Sci., Part A: Polym. Chem.* **2001**, *39*, 4294. (d) Xiao, D.; Wirth, M. J. *Macromolecules* **2002**, *35*, 2919. (e) Lopinski, G. P.; Wayner, D. D. M.; Wolkow, R. A. *Nature* **2000**, *406*, 48. (f) Tong, X.; DiLabio, G. A.; Clarkin, O. J.; Wolkow, R. A. *Nano Lett.* **2004**, *4*, 357. (g) Tong, X.; DiLabio, G. A.; Wolkow, R. A. *Nano Lett.* **2004**, *4*, 979.

(6) (a) Buchanan, A. C., III; Britt, P. F.; Thomas, K. B.; Biggs, C. A. *J. Am. Chem. Soc.* **1996**, *118*, 2182. (b) Buchanan, A. C., III; Britt, P. F. *J. Anal. Appl. Pyrolysis* **2000**, *54*, 127. (c) Britt, P. F.; Buchanan, A. C., III; Malcolm, E. A. *Energy Fuels* **2000**, *14*, 1314. (d) Buchanan, A. C., III; Britt, P. F.; Skeen, J. T.; Struss, J. A.; Elam, C. L. *J. Org. Chem.* **1998**, *63*, 9895. (e) Buchanan, A. C., III; Britt, P. F.; Koran, L. J. *Energy Fuels* **2002**, *16*, 517. (f) Britt, P. F.; Buchanan, A. C., III; Malcolm, E. A. *Energy Fuels*

2000, *14*, 1314. (g) Buchanan, A. C., III; Britt, P. F.; Thomas, K. B. *Energy Fuels* **1998**, *12*, 649.

(7) Kidder, M. K.; Britt, P. F.; Zhang, Z.; Dai, S.; Buchanan, A. C., III *Chem. Commun.* **2003**, 2804.

(8) Buchanan, A. C., III; Biggs, C. A. *J. Org. Chem.* **1989**, *54*, 517.

(9) (a) Poutsma, M. L.; Dyer, C. W. *J. Org. Chem.* **1982**, *47*, 4903. (b) Gilbert, K. E.; Gajewski, J. J. *J. Org. Chem.* **1982**, *47*, 4899.

(10) Buchanan, A. C., III; Kidder, M. K.; Britt, P. F. *J. Am. Chem. Soc.* **2003**, *125*, 11806.

(11) Godfrey, I. M.; Sargent, M. V.; Elix, J. A. *J. Chem. Soc., Perkin Trans. 1* **1974**, 1353.

(12) (a) Vasudevan, A.; Qian, Y.; Vogt, A.; Blaskovich, M. A.; Ohkanda, J.; Sebti, S. M.; Hamilton, A. D. *J. Med. Chem.* **1999**, *42*, 1333. (b) Ohe, T.; Miuaura, T.; Suzuki, A. *J. Org. Chem.* **1993**, *58*, 2201.

(13) Snyder, H. R.; Werber, F. X. *Org. Synth.* **1995**, *Coll. Vol. 3*, 798.

(14) DuPriest, M. T.; Schmidt, C. L.; Kuzmich, D.; Williams, S. B. *J. Org. Chem.* **1986**, *51*, 2021.

(15) Takaki, K.; Okada, M.; Yamada, M.; Negoro, K. *J. Org. Chem.* **1982**, *47*, 1200.

(16) Burger, A.; Mosettig, E. *J. Am. Chem. Soc.* **1936**, *58*, 1857.

(17) The related *p*-methoxy group is also known to be a mildly stabilizing substituent for benzyl radicals. Creary, X. *J. Org. Chem.* **1980**, *45*, 280.

(18) Termination can occur by radical coupling and/or disproportionation. We have noted previously that termination by coupling of two immobilized benzylic radicals on the surface is inhibited by conformational strain in the resulting diattached product.[8] In some cases, such as pyrolysis of silica-immobilized bibenzyl, this can lead to dramatically altered product compositions compared with fluid phases. See, for example: Buchanan, A. C., III; Dunstan, T. D. J.; Douglas, E. C.; Poutsma, M. L. *J. Am. Chem. Soc.* **1986**, *108*, 7703. In the ≈DPP chemistry, chain termination typically occurs through benzyl radical coupling involving gas-phase benzyl radicals,[8] as is the current case for ≈DPP with the ≈FL spacers. However, in the case of the ≈DHP and ≈TET spacers, some chain termination could conceivably occur through disproportionation of adjacent spacer radicals.

(19) Franz, J. A.; Alnajar, M. S.; Barrows, R. D.; Kaisaki, D. L.; Camioni, D. M.; Suleman, N. K. *J. Org. Chem.* **1986**, *51*, 1446.

(20) (a) Liu, C. C.; Maciel, G. E. *J. Am. Chem. Soc.* **1996**, *118*, 5103. (b) Chuang, I. S.; Maciel, G. E. *J. Phys. Chem. B* **1997**, *101*, 3052.

(21) Sigman, M. E.; Read, S.; Barbas, J. T.; Ivanov, I.; Hagaman, E. W.; Buchanan, A. C., III; Dabestani, R.; Kidder, M. K.; Britt, P. F. *J. Phys. Chem. A* **2003**, *107*, 3450.

(22) Slightly higher coverages could be achieved on the [100] surface, which has 3.95 geminal silanol sites nm^{-2} (7.90 SiOH nm^{-2}) 0.5 nm apart in a square array.[20,21]

(23) Coote, M. L.; Collins, M. A.; Radom, L. *Mol. Phys.* **2003**, *101*, 1329.

(24) Cacciapaglia, R.; Di Stefano, S.; Mandolini, L. *Acc. Chem. Res.* **2004**, *37*, 113.